JOURNAL OF GEOPHYSICAL RESEARCH, VOL. 106, NO. A10, PAGES 21,083–21,093, OCTOBER 1, 2001

Polar cusp and vicinity under strongly northward interplanetary magnetic field on April 11, 1997: Observations and MHD simulations

G. Le,[1,2] J. Raeder,[1] C. T. Russell,[1] G. Lu,[3] S. M. Petrinec,[4] and F. S. Mozer[5]

Abstract. We present a correlative case study of the solar wind interaction with the magnetosphere using in situ observations of the polar cusp and surrounding regions, ground-based and low-altitude spacecraft polar cap observations, and global MHD simulations during an extended period of strongly northward interplanetary magnetic field (IMF) on April 11, 1997. Within this extended period of strongly northward IMF, the Polar spacecraft entered a region with magnetosheath-like plasma and field lines above the polar cusp. Data from multiple instruments on Polar showed that the observed signatures can be interpreted as Polar entering the reconnection layer and crossing the current layer associated with it. The magnetosheath-like field lines encountered by Polar have just reconnected poleward of the polar cusp in the north. The reversed ionospheric convection patterns derived from the assimilative mapping of ionospheric electrodynamics (AMIE) technique show the reversed convection over the polar cap due to high-latitude reconnection throughout the whole interval. MHD simulations were performed using solar wind parameters observed by Wind, supporting the cusp reconnection interpretation.

1. Introduction

The polar cusp and surrounding region is of great interest in the study of the solar wind-magnetosphere interaction since it is the region through which the solar wind plasma has direct access to the low altitudes [*Heikkila and Winningham*, 1971; *Frank*, 1971]. *Dungey* [1961] first predicted that, when the interplanetary magnetic field (IMF) is northward, the interaction of the solar wind with the Earth's magnetosphere will cause the interplanetary field lines to merge with the tail lobe magnetic field lines at two points poleward of both the northern and southern polar cusps. *Russell* [1972] discussed the consequences of Dungey's model and found that modification was necessary to be consistent with observations of the open magnetotail regardless of the sign of IMF *Bz*. Specifically, Russell stressed that the same interplanetary field lines could not be reconnected above both cusps at the same time, in particular, if the interplanetary magnetic field is not exactly northward. In the modified scenario the IMF line is convected to the magnetopause where it merges at a point poleward above one cusp and forms two newly reconnected field lines: the one with both ends in the solar wind is convected away from the Earth by the solar wind, the one connected to the polar ionosphere and the solar wind is dragged toward the low-latitude and soon pulled back to the tail by the solar wind. Although the high-latitude merging does not transport magnetic flux between dayside magnetosphere and magnetotail (in contrast to the case for southward IMF), it does induce plasma convection over the polar cap. The modified reconnection model predicted that for northward IMF the merging of the interplanetary field lines with the lobe field lines drives sunward plasma convection over the polar cap, opposite to the convection direction driven by the dayside reconnection for southward IMF.

Since Dungey's reconnection model was proposed, there is mounting evidence that provides observational support to high-latitude reconnection under northward IMF, although the dayside reconnection under southward IMF attracted most attention owing to the availability of in situ observational data. Polar cap observations have been used to infer processes occurring at the magnetopause boundary in studies of the solar wind interaction with the magnetosphere. *Maezawa* [1976] deduced the polar cap convection pattern in a detailed statistical study and confirmed that sunward plasma convection is induced in the polar cap under northward IMF conditions, implying that the driving mechanism is reconnection poleward of the cusp region. Sunward polar cap convection is also seen in low-altitude cusp observations under northward IMF at both the northern and the southern polar caps [*Burke et al.*, 1979; *Reiff*, 1982; *Zanetti et al.*, 1984; *Woch and Lundin*, 1992]. Meanwhile, high-latitude reconnection has been inferred from the interpretation of plasma observations of the low-latitude boundary layer [*Paschmann et al.*, 1990; *Song and Russell*, 1992; *Song et al.*, 1993; *Le et al.*, 1994, 1996]. Before the Polar spacecraft, direct evidence of high latitude reconnection from in situ observations was reported from two data sets, from ISEE data by *Gosling et al.* [1991, 1996] and from Hawkeye data by *Kessel et al.* [1996], where the properties of plasma flow were found to agree qualitatively with the predictions of the reconnection model.

The Polar spacecraft makes in situ observations of the northern cusp and surrounding region at altitudes ≥ 6 R_E, well above the low-altitude region extensively probed by DMSP. Under normal solar wind conditions the Polar spacecraft stays well inside the magnetopause near its apogee (~9 R_E). During its first 3 years of operation, Polar has

[1]Institute of Geophysics and Planetary Physics, University of California, Los Angeles.
[2]Now at Laboratory for Extraterrestrial Physics, NASA, Goddard Space Flight Center, Greenbelt, Maryland.
[3]High Altitude Observatory, National Center for Atmospheric Research, Boulder, Colorado.
[4]Space Physics Laboratory, Lockheed Martin Advanced Technology Center, Palo Alto, California.
[5]Space Sciences Laboratory, University of California, Berkeley.

Paper number 2000JA900091.
0148-0227/01/2000JA900091$09.00

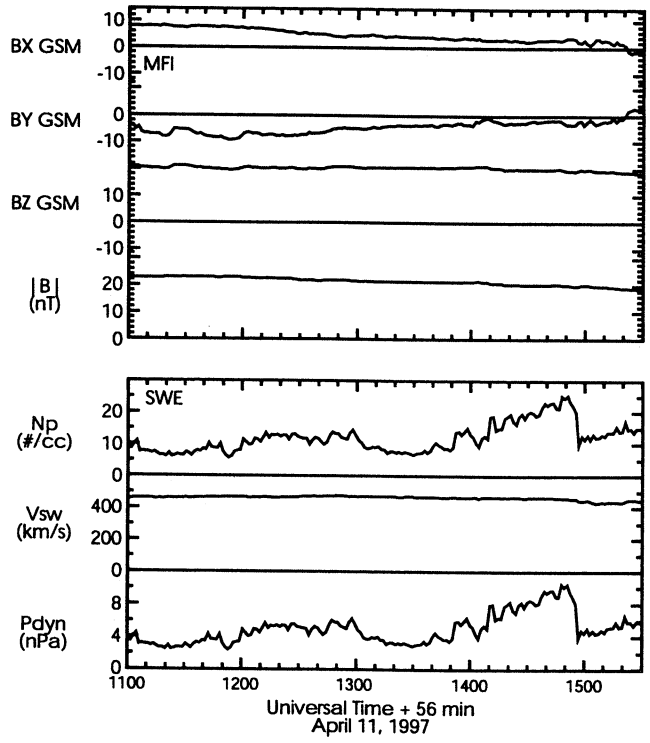

Figure 1. The Wind solar wind and interplanetary magnetic field (IMF) data from 1100 to 1530 UT on April 11, 1997. The time is shifted by 56 min to account for the travel time from the Wind spacecraft to the Earth.

2. Solar Wind and IMF Observations

The Wind solar wind [*Ogilvie et al.*, 1995] and IMF data [*Lepping et al.*, 1995] for the time period of interest are shown in Figure 1 from 1130 to 1550 UT, April 11, 1997. The time has been shifted by 56 min to account for the travel time from the Wind spacecraft (located ~230 R_E sunward) to the Earth, timed by the sharp pressure drop at 1456 UT (at Earth) observed in both the Wind solar wind data and the Polar magnetic field data. During this period the IMF was quite steady with a large magnetic field strength and a strongly northward *Bz* component (~ +20 nT). The IMF clock angle gradually decreased from being ~20° to 6° from the due north direction. The solar wind velocity was ~470 km/s for the interval. The solar wind dynamic pressure initially was steady at ~4-6 nPa, started to increase at ~1400 UT (at Earth), reached a maximum of ~10 nPa at 1450 UT (at Earth), and sharply dropped to ~4 nPa at 1456 UT (at Earth).

3. Cusp and Vicinity Observations from Polar

The Polar spacecraft was moving toward its apogee from below the cusp latitudes to well above the cusp latitudes during the period of interest. Figure 2 shows the Polar orbit as the distance from the Earth-Sun line versus the distance along it. The polar orbit plane was roughly at 1330 LT. Also shown in Figure 2 is the magnetopause position predicted by the *Petrinec and Russell* [1993] empirical model for the solar wind conditions at 1450 UT, when the magnetopause was most compressed at the maximum solar wind dynamic pressure (10 nPa) for this interval. On the basis of magnetopause model prediction, Polar should have stayed inside the magnetopause for the entire time period of interest.

entered the magnetosheath only when the magnetosphere was extremely compressed such as during the May 4, 1998, event [*Russell et al.*, 2000a]. Nevertheless, under moderately high solar wind dynamic pressure such as on May 29, 1996, Polar came close to the magnetopause and observed the magnetosheath-like plasma entering the magnetosphere through post-cusp reconnection [*Russell et al.*, 1998]. Recently, controversy arose over the site of reconnection for northward IMF as *Fuselier et al.* [1997] reported that the reconnection could occur on occasion equatorward of the cusp between the nearly parallel magnetosheath and dayside magnetospheric field based on Polar/TIMAS data.

On April 7, 1997, the SOHO spacecraft observed a large eruption on the Sun. The ejected solar material, or coronal mass ejection (CME), arrived at the Earth on April 10 and caused strong auroral and geomagnetic activity and intensified magnetospheric current systems on April 10-11. The Wind spacecraft observed that the CME started with a strong southward IMF. At ~0600 UT (at Wind) on April 11 the magnetic field turned to a strongly northward direction that lasted for more than 12 hours. Within this extended period of strongly northward IMF, the Polar spacecraft passed through the northern cusp region at altitudes of ~6 R_E and then went into a region of dense magnetosheath-like plasma above the polar cusp [*Fuselier et al.*, 2000; *Russell et al.*, 2000b]. While both Fuselier et al. and Russell et al. interpreted the plasma signatures from Polar/TIMAS data in terms of reconnection, controversy arose on the site of the reconnection. In this paper, we present additional evidence based on in situ observations from the Polar spacecraft, ionospheric convection patterns derived from the assimilative mapping of ionospheric electrodynamics (AMIE) technique, as well as global MHD simulations to support the interpretation in terms of reconnection poleward of the cusp region.

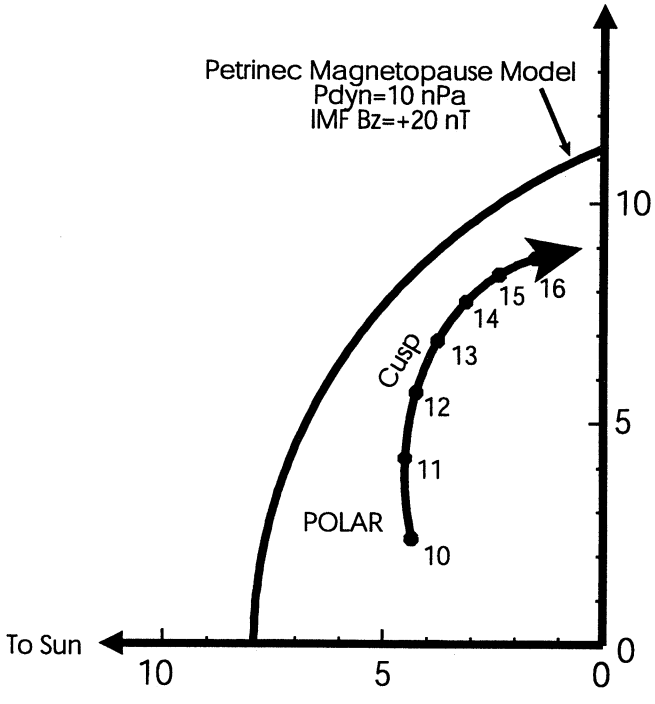

Figure 2. Polar orbit as the distance from the Earth-Sun line versus the distance along it. The Polar orbit plane was roughly at 1330 LT. The magnetopause position is predicted by *Petrinec and Russell* [1993] empirical model using the maximum solar wind dynamic pressure (10 nPa) in the period of interest.

Plate 1 shows the Polar key parameter data for the same time period as in Figure 1, including the magnetic field data (top) [*Russell et al.*, 1995], electron density and average energy from hot plasma analyzer (Hydra) (bottom) [*Scudder et al.*, 1995], and proton densities for three energy channels and the full energy range from the Toroidal Imaging Mass-Angle Spectrograph (TIMAS) [*Shelley et al.*, 1995]. In Plate 1 (top) is also shown the predicted magnetic field from *Tsyganenko* [1996] empirical model with observations from Wind as input parameters. Typical polar cusp signatures are evident in the first half of the data in Plate 1, occurring within the period with moderate solar wind dynamic pressure. The magnetic field strength decreased as the spacecraft moved to higher altitude. At ~1130 UT, Polar went into the cusp region characterized by enhanced plasma density due to the entering magnetosheath plasma. The magnetic field strength became more depressed in comparison with the model, consistent with the enhanced plasma density. The plasma in the cusp region has lower energy than that in the magnetosphere equatorward of the cusp. Overall the field strength continued to decrease. At ~1152 UT the magnetic field started to show enhanced fluctuations. Coincidentally, the ion density in the medium key parameter energy range (0.37-3.3 keV/*e*) increased to a new level. At ~1300 UT, Polar entered the lobe region poleward of the cusp.

A more interesting feature occurred poleward of the cusp region when the solar wind dynamic pressure started to increase and the magnetopause was pushed inward by the enhanced dynamic pressure. During the interval ~1430-1452 UT, Polar went into a dense plasma region with magnetosheath-like properties. The plasma in this region is magnetosheath-like in terms of its density and temperature values. (Please note that TIMAS instrument was saturated here, and thus the ion density was underestimated.) Meanwhile the magnetic field rotated from lobe-like field orientation outside the region to magnetosheath-like orientation for strongly northward IMF inside the region. However, the Polar spacecraft did not move into the magnetosheath proper during this interval based on the observation of plasma bulk velocity. If Polar had gone into the magnetosheath proper above the cusp region, the plasma bulk flow would have had a velocity around $0.6V_{sw}$, or ~280 km/s at Polar location based on the gas dynamic model of the magnetosheath [*Spreiter et al.*, 1966] and the global MHD simulation [*Raeder et al.*, 1997]. However, the velocity data from Polar/TIMAS observations indicate nearly stagnant plasma flow in this region (not shown). We calculated the **ExB** drift velocity using the Polar electric field [*Harvey et al.*, 1995] and the magnetic field data. The 1-min-averaged plasma bulk velocity in the region with magnetosheath-like plasma is ~78 km/s, well below the expected plasma velocity in high latitude magnetosheath, as shown in Figure 3. On the basis of these observations we believe that the Polar spacecraft was not in the undisturbed magnetosheath proper when it observed the magnetosheath-like plasma and field.

Recently, *Fuselier et al.* [2000] examined the Polar/TIMAS observations of electron and ion distribution functions for this interval and found that the angular distribution of the magentosheath-like plasma contained two components: the incoming solar wind beam (parallel propagation) and a reflected component (antiparallel propagation) that had higher-energy and lower flux, indicating that the spacecraft was on a magnetic field line that had one foot in the northern ionosphere, thus was not in the undisturbed magnetosheath. Fuselier et al. interpreted the observed electron and ion signatures in terms of reconnection of nearly parallel magnetospheric and magnetosheath field lines at a site below the cusp. However, *Russell et al.* [2000] offered a simpler interpretation that is consistent with the

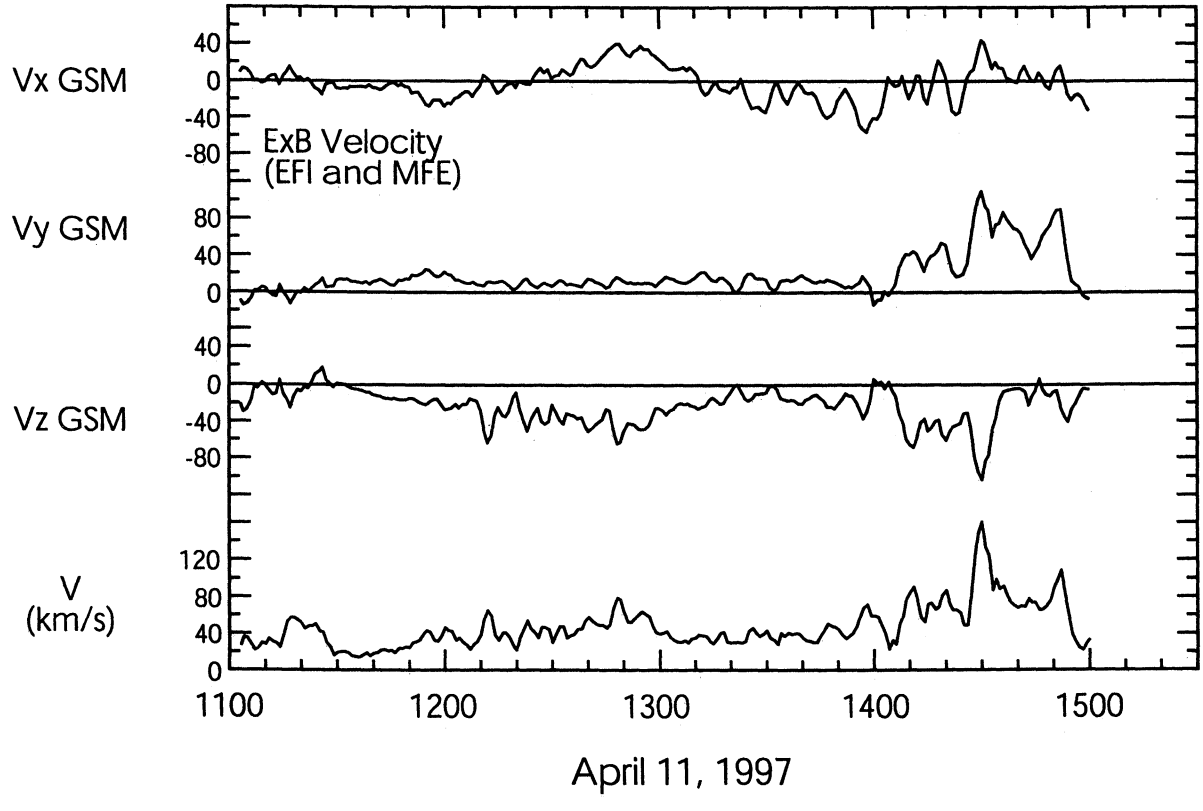

Figure 3. The **ExB** drift velocity deduced from the Polar electric field and the magnetic field data for the same time period as in Figures 1 and 3.

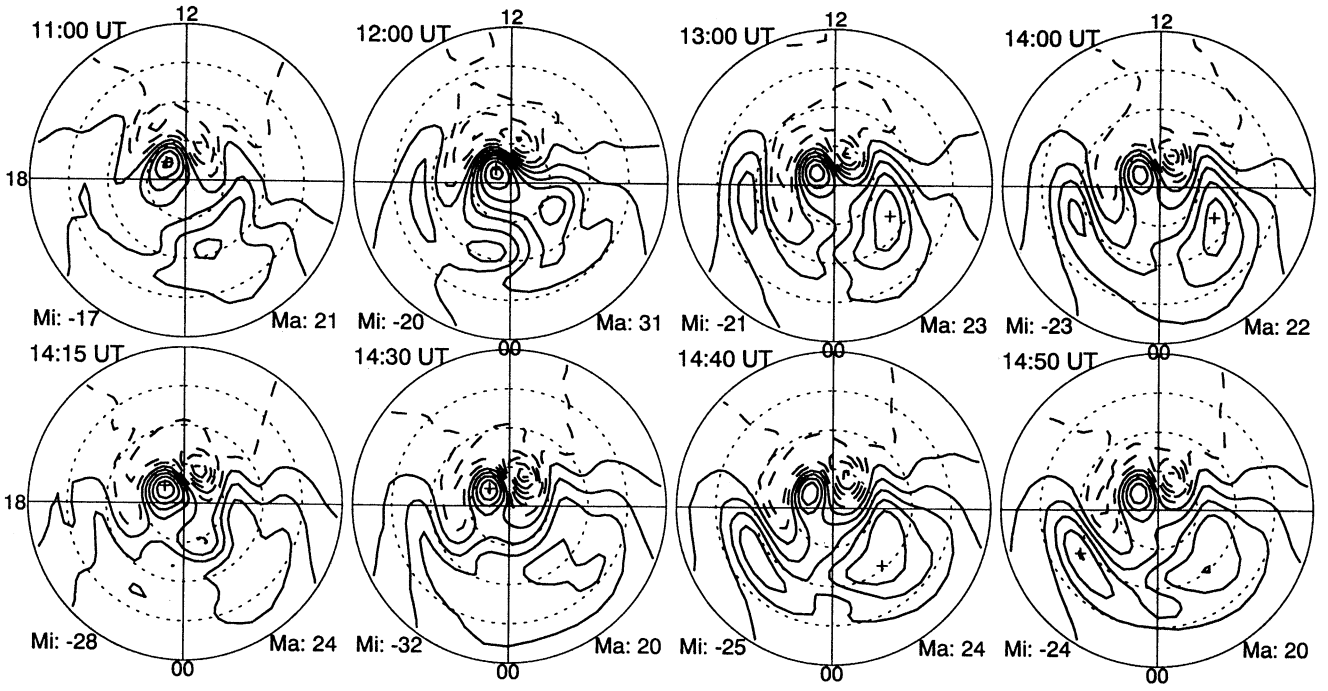

Figure 4. Representative snapshots of the ionospheric convection patterns taken at times 1100 (when Polar was in dayside magnetosphere equatorward of cusp), 1200 (when Polar was in the cusp region), 1300 (when polar was near the poleward boundary of the cusp and just entered the tail lobe), 1400, and 1415 UT (when Polar was in the tail lobe), as well as 1430, 1440, and 1450 UT (when Polar was in the region with magnetosheth-like plasma). Dashed contours represent negative electric potentials and solid contours for positive electric potentials, with a contour interval of 5 kV. The plus and minus signs indicate the locations of the most positive and negative potentials.

current paradigm of reconnection for northward IMF. The observed plasma and field signatures can be interpreted as Polar entering into a layer of reconnection that occurred poleward of the cusp region and crossing the current layer associated with this reconnection layer. The magnetosheath-like field lines encountered by Polar have just reconnected poleward of the polar cusp in the north. The magnetosheath-like plasma seen by Polar came from the magnetosheath through the high-latitude reconnection site.

4. Polar Cap Convection Patterns From AMIE Model

Reconnection applies a stress to the outer magnetosphere that is transmitted to the ionosphere via field-aligned currents. Thus the convection pattern of the polar cap plasma is controlled by the reconnection process, and polar cap plasma convection patterns in turn provide information on the reconnection process at the magnetopause. One way to verify the reconnection site for this interval is to examine the simultaneous ionospheric convection pattern. When reconnection occurs poleward of the cusp region for northward interplanetary field, it drives sunward plasma convection over the polar cap [*Maezawa*, 1976; *Russell*, 1972; *Reiff*, 1982]. If the reconnection site is equatorward of the cusp between the magnetosheath field and dayside magnetospheric field, it causes the erosion of the dayside magnetosphere and drives a antisunward convection over the polar cap. The assimilative mapping of ionospheric electrodynamics (AMIE) technique [*Richmond and Kamide*, 1988] has proven to be very useful in studying the ionospheric convection [*Knipp et al.*, 1991, *Lu et al.*, 1994; *Ridley et al.*, 1997]. It can provide snapshots of ionospheric convection patterns by combining simultaneous global ground- and space-based observations.

We have used the AMIE technique to derive the ionospheric convection patterns for the period from 1100 to 1500 UT, covering the entire interval of interest from Polar entering the cusp region till its exit from the region with magnetosheath-like plasma. We find that the polar cap plasma convection consistently shows the reversed two-cell convection patterns expected for high-latitude reconnection throughout the interval. Figure 4 shows a few selected representative snapshots of the ionospheric convection patterns taken at times 1100 UT (when Polar was in dayside magnetosphere equatorward of cusp), 1200 UT (when Polar was in the cusp region), 1300 UT (when polar was near the poleward boundary of the cusp and just entered the tail lobe), 1400 and 1415 UT (when Polar was in the tail lobe), as well as 1430, 1440, and 1450 UT (when Polar was in the region with magnetosheath-like plasma). The dashed contours represent negative electric potentials, or clockwise plasma convection. The solid contours represent positive potentials, or counterclockwise plasma convection. All the snapshots for the entire period of interest show a reversed two-cell convection with the morning cell clockwise and afternoon cell counterclockwise. Thus the plasma was convected sunward over the polar cap. This indicates that high-latitude reconnection was going on throughout the whole interval. This conclusion is consistent with the in situ Polar observation of the reconnection layer poleward of the cusp.

5. Comparison With Global MHD Simulations

In order to obtain a global picture of the reconnection geometry during this event and to further understand the prevailing physical processes we performed a global simulation of this event. Briefly, our model solves the three-dimensional MHD equations for the entire magnetosphere, from upstream of the bow shock to the distant tail, excluding a spherical region surrounding Earth of 3.5 R_E radius. Inside

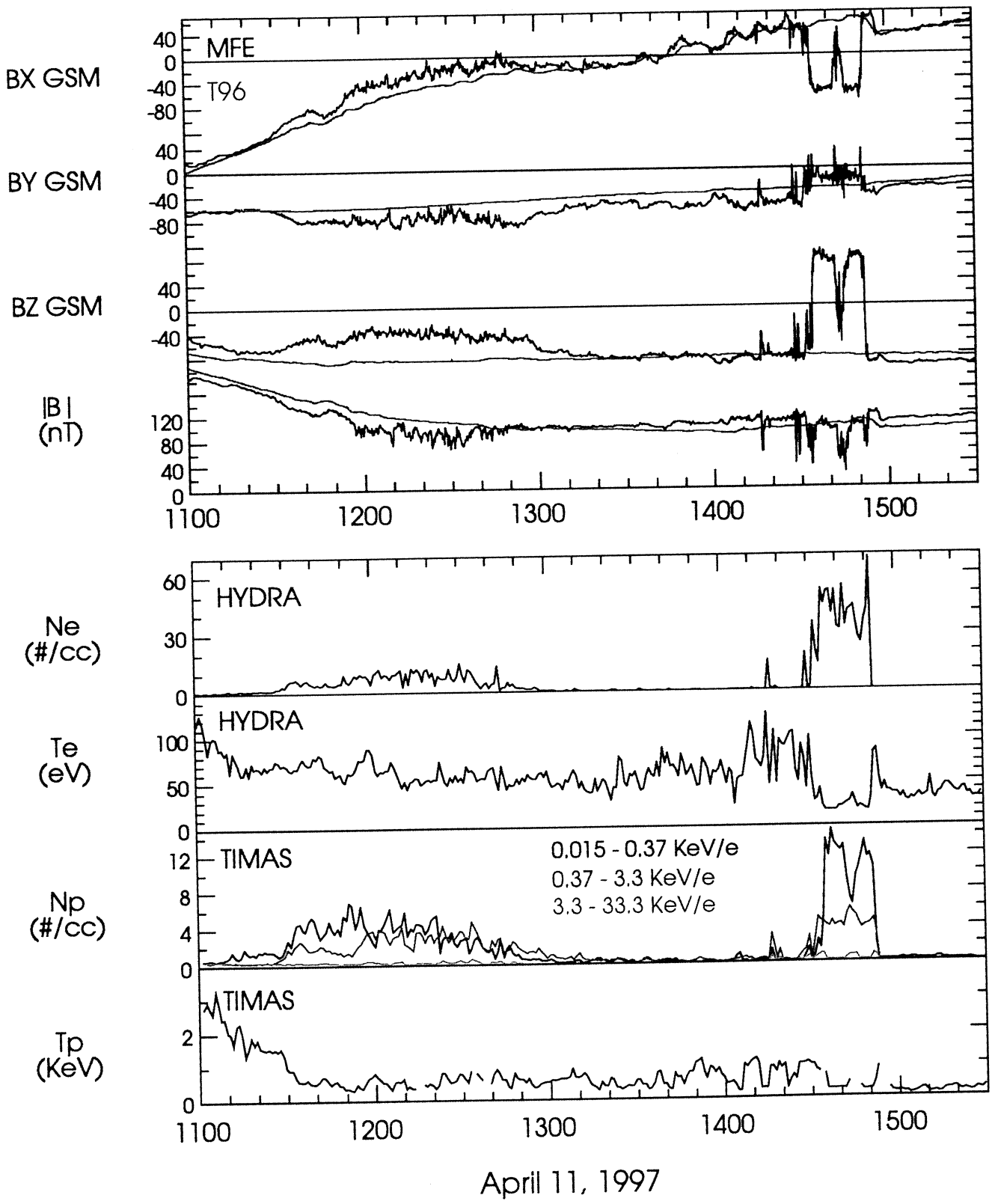

Plate 1. Polar key parameter data for the same time period as in Figure 1, including (top) the magnetic field data, (bottom) electron density and energy from Hot Plasma Analyzer (Hydra, courtesy of J. Scudder), and proton densities for three energy channels and full range energy from Toroidal Imaging Mass-Angle Spectrograph (TIMAS, courtesy of W. K. Peterson).

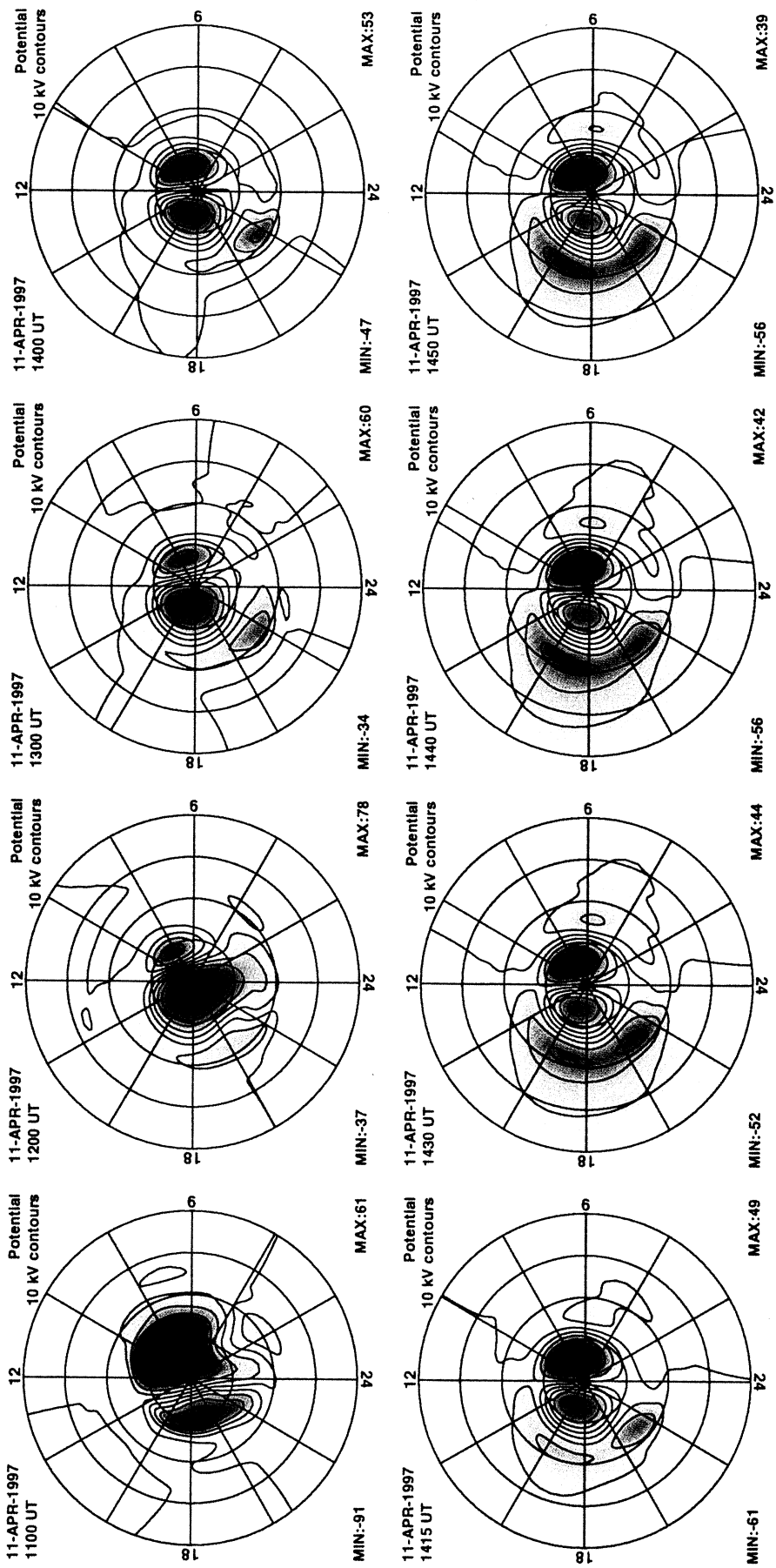

Plate 2. Ionospheric convection patterns obtained by the global MHD simulation at the same times as the observationally derived AMIE patterns shown in Figure 4.

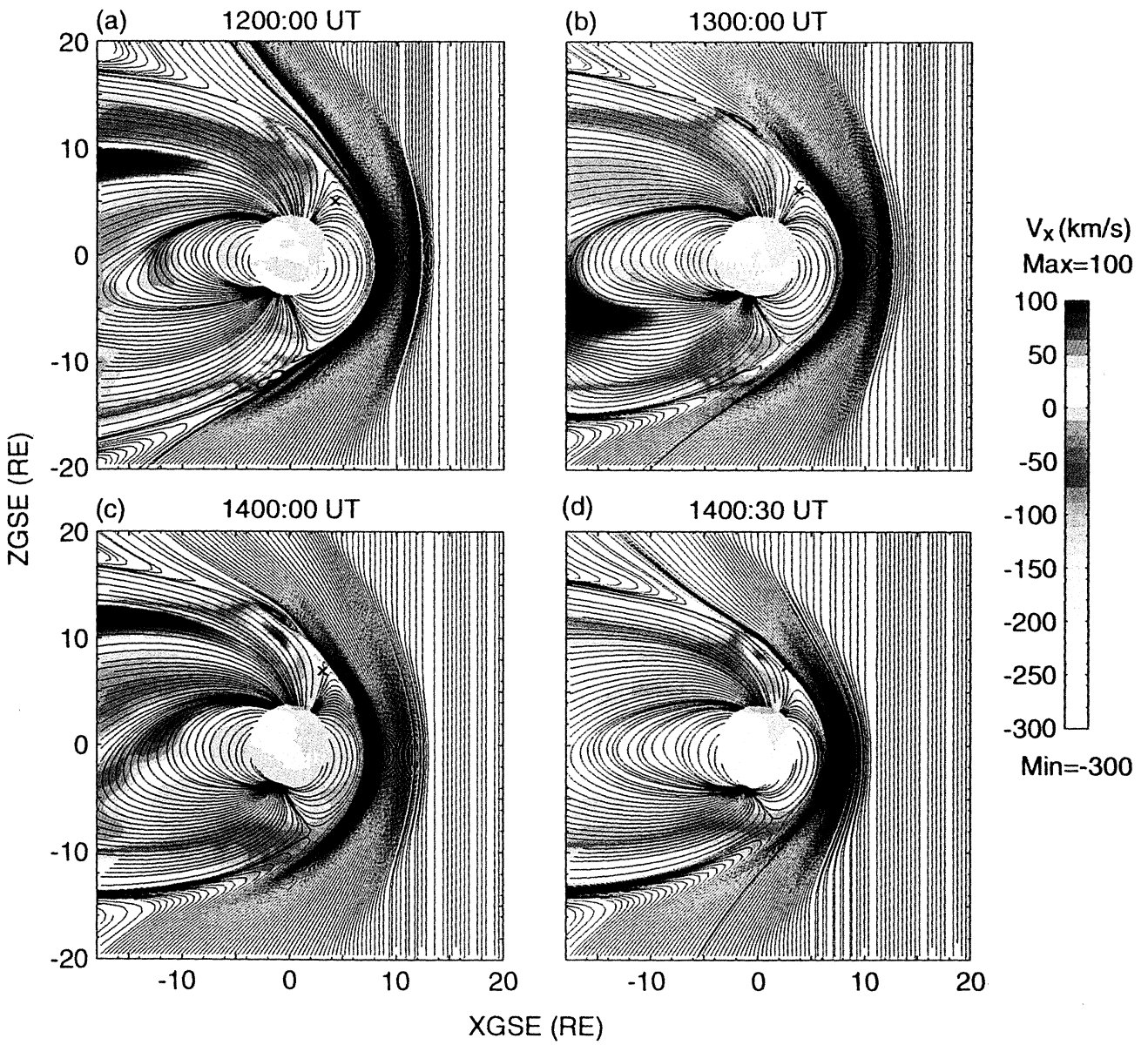

Plate 3. Cuts from the simulation in the XZ plane (in GSE) through the Polar position (YGSE=3.6 R_E) at four different times (a) 1200, (b) 1300, (c) 1400, and (d) 1430 UT. The color coding shows the X component of the plasma bulk velocity and the lines are tangential to the field direction. Note that these lines are not field lines or projections thereof but rather the lines that are tangential to (Bx, Bz) within the YGSE=3.6 R_E plane. The cross marks the Polar position at corresponding times.

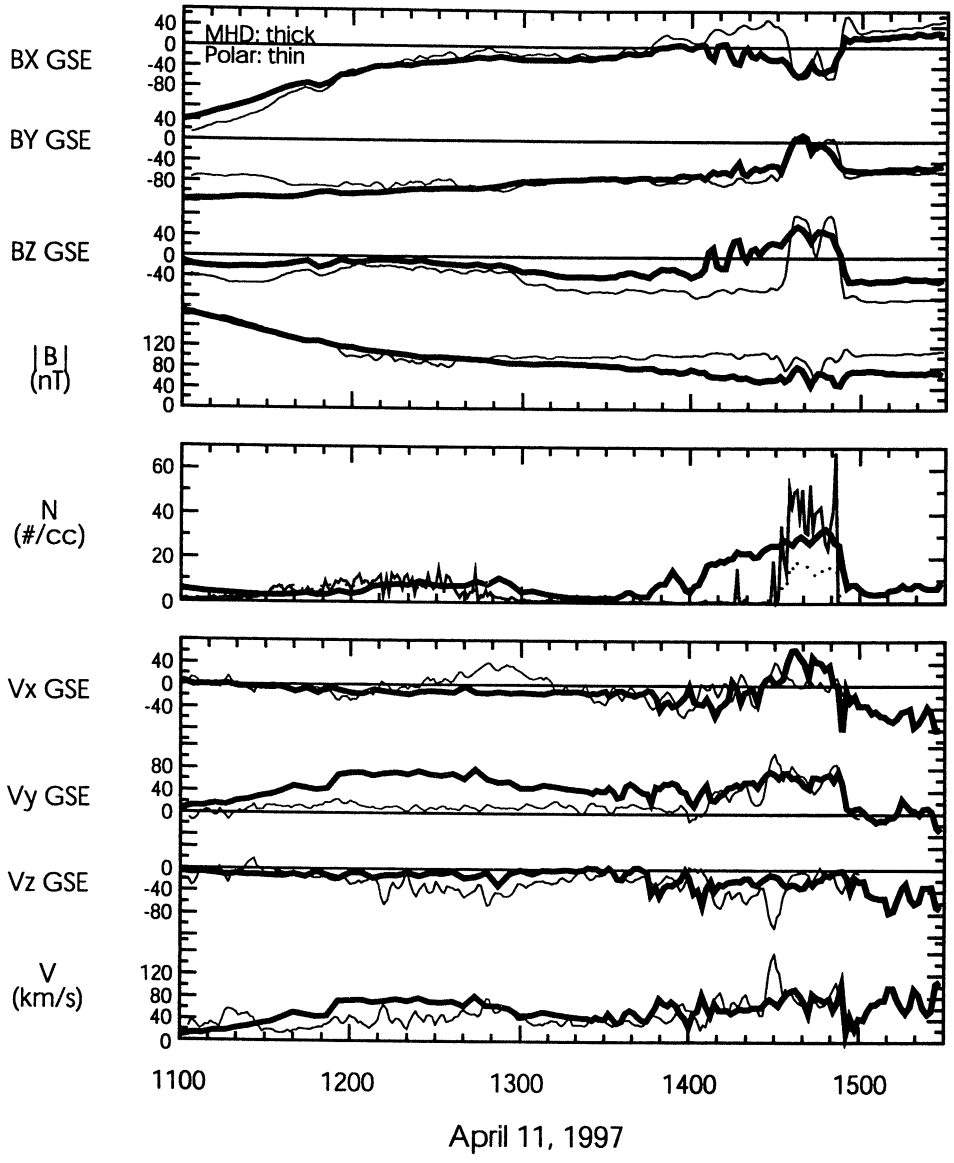

Figure 5. The thick traces are magnetic field components, magnetic field magnitude, plasma density, and bulk velocity along the Polar trajectory from MHD global simulations. The thin traces are Polar observations.

this region, the MHD equations are not solved, but a static dipole field is assumed. Field-aligned currents (FACs) are mapped from the magnetosphere along these dipole field lines into the ionosphere where they are used to calculate the ionospheric potential. The ionospheric potential is then used as a boundary condition for the MHD variables at the 3.5 R_E surface, closing the electrodynamic magnetosphere-ionosphere coupling circuit. A more detailed description of the model can be found in the works of *Raeder et al.* [1997, 1998] and *Raeder* [1999].

The simulation begins at 0800 UT. The IMF is first kept due southward for 1 hour in order to let a magnetosphere develop from the initial conditions. After that we use the measured solar wind IMF and plasma moments as input for the model. As a first test of the validity of the model, we compare time traces of the MHD variables with the observations. These are shown in Figure 5. From top to bottom we compare the field components, field magnitude, plasma density, and velocity. The thin lines are the observed values while the thick lines are time traces taken from the simulation at the Polar position. No attempt was made to vary the Polar position to improve the comparison. The simulation clearly shows the density enhancements and field deflections of the cusp. During the lobe intervals the field and plasma values also closely match the observed values. The simulation also shows Polar entering a region of magnetosheath-like plasma and fields. However, the simulated entry is ~30 min earlier than the observed entry. Several reasons may account for this difference, but most likely it is due to the limited resolution of the simulation, which is of the order of ~0.5 R_E near where Polar is. However, inaccuracies of the solar wind propagation from Wind to the simulation box (Wind was 229 R_E upstream of Earth and 23 R_E off the Sun-Earth line) and lack of knowledge of the true solar wind mass density (due to He^{++}) may also play a role. Despite this early boundary crossing in the simulations the exit of this region is sharply defined in both the data and the simulations in response to the sudden drop of the solar wind dynamic pressure, and the field and plasma time series match extremely well during the 1430 to 1500 UT time period. Thus the simulation replicates the key observation during this period, i.e., the crossings of the magnetopause current sheet, the magnetosheath-like plasma properties, and the stagnant flows in this region. This gives us

confidence that the simulation is a very close image of reality and that the relevant physical processes are properly included.

A second reality check is provided by the ionospheric convection patterns. Plate 2 shows patterns obtained by the simulation at the same times as the observationally derived AMIE patterns shown in Figure 4. Although there are differences in the details, the convection patterns are generally the same. In particular, the simulation shows the same two reverse convection cells sitting over the magnetic pole as AMIE. Thus convection over the pole is sunward, which can only be explained by the reconnection process between lobe and northward IMF field lines. A notable difference between the AMIE and the simulation covection potentials is the value of the cross polar cap potential that is about twice as high in the simulation results compared to the AMIE estimates. Similar differences have been found in earlier comparisons [*Raeder et al.*, 1998] and are currently not well understood. Possible causes include an underestimate of the potential drops by AMIE, too rapid reconnection rates in the simulation, or inaccurate calculation of the ionospheric Hall and Pedersen conductances in the simulation.

Plate 3 shows cuts from the simulation in the XZ plane (in GSE) through the Polar position, i.e., at YGSE = 3.6 R_E, at four different times, (a) 1200 UT, (b) 1300 UT, (c) 1400 UT and (d) 1440:30 UT. The color coding shows the X component of the plasma bulk velocity and the lines are tangential to the field direction, i.e., these lines are not field lines or projections thereof, but indicate the local direction of the field in the YGSE=3.6 R_E plane. The cross marks the Polar position. Clearly, Polar moves from the magnetosphere equatorward of the cusp, through the cusp, and then to a position immediately tailward of the cusp and near the magnetopause. Here it remains close to, or within the current layer after 1430 UT. Tailward of Polar lies a reconnection site where lobe field lines reconnect with IMF field lines. Note that Polar never gets onto undisturbed magnetosheath field lines with both ends connected to the solar wind. Although it crosses the current sheet, it remains on field lines that are of IMF origin, but have already reconnected at a location that is ~5 R_E tailward of Polar. Thus one would not expect that Polar observes undisturbed magnetosheath plasma, but rather a plasma population that is substantially altered by the reconnection process. We will come back to this point later in our discussion.

It is also noteworthy that the reconnection site is not stationary but moves back and forth while shedding small plasmoid or flux rope like features. Such an unsteady reconnection process has already been observed in earlier simulations for northward IMF [*Berchem et al.*, 1995], and there is also observational evidence from Hawkeye observations [*Kessel et al.*, 1996]. Recalling the Polar observations within the polar cusp region, the magnetic field started to show enhanced fluctuations at ~1152 UT and lasted till the spacecraft exited the polar cusp at ~1300 UT in contrast with the lower latitude part of the cusp region from ~1130 to 1152 UT (Plate 1). Since the lower-latitude part of the cusp field lines map to the low-latitude boundary layer at subsolar region and the higher-latitude part of the cusp field lines map to the high-latitude boundary layer, the enhanced magnetic fluctuations are consistent with the interpretation that there was ongoing unsteady reconnection poleward of the cusp region to which the higher-latitude part of the cusp field lines maps.

The simulation also shows a layer of sunward flow that is located just inside the magnetopause and sunward (equatorward) of the reconnection site. Such a layer is expected from local simulation [*Scholer*, 1989] of asymmetric reconnection, i.e., where the plasma density, plasma β, and magnetic field strength are substantially different on either side of the current sheet. In that situation, strong flows emanate from the X line on the side which has the higher Alfven speed. This phenomenon is also present in Plates 3a-3d, and Polar observed such sunward flows before it entered the magnetopause between ~1310 and 1420 UT (see Figures 3 and 5). Note that the magnitude of the sunward flows is identical in the data and in the simulation. Also both in the data and in the simulation the flows are variable on a timescale of ~5-10 min. This can easily be understood in view of the fact that the reconnection site, and most likely also the reconnection rate, are variable as well. These sunward flows are thus strong evidence that postcusp reconnection indeed occurred during this interval, for otherwise, they would be difficult to explain, whereas the simulation gives a straightforward explanation.

6. Discussion

In the this paper, we presented a case with in situ observation from Polar and simultaneous polar cap convection patterns deduced by the AMIE model from ground-based and low-altitude spacecraft data and compared the observations with global MHD simulation model. The IMF data from Wind show that the IMF Bz turned to strongly northward at ~0700 UT on the Earth and lasted for more than 12 hours. In the 4-hour period starting from 1100 UT (before Polar went into the cusp region until it exited from the reconnection layer) the AMIE model shows consistently that the plasma had a sunward convection over the polar cap for the entire period (Figure 4). The reversed convection patterns throughout the whole period imply that the same driving process was responsible for the observed plasma convection and the driving process was the reconnection between the interplanetary field lines and the lobe field lines. Further supporting evidence for the ongoing reconnection is provided from in situ observations of Polar in the latter part of this period as the spacecraft encountered the layer of newly reconnected field lines due to the increasing solar wind dynamic pressure. Significant magnetosheath plasma was seen on the reconnected magnetic field lines (Plate 1). The plasma flow in the reconnection layer is nearly stagnant with a speed much less than the solar wind speed (Figure 3).

The MHD simulation gives us a global picture of the solar wind interaction with the magnetosphere under strongly northward IMF. The quantitative comparison with the MHD model provides further support to the interpretation of the data. Ongoing reconnection poleward of the cusp is confirmed in the MHD simulations (Plates 2 and 3). The magnetic and plasma properties seen by Polar spacecraft are very similar to those predicted by the global MHD simulations (Figure 5). The location of polar cusp region from MHD simulations agrees quantitatively with Polar observations (Figure 5 and Plate 3). The location of the reconnection layer is also in agreement with the Polar observations except that the layer is much thinner than that expected from the simulation model. The reason may be that the sharp feature is smoothed out in the MHD simulations owing to limited resolution in space and time in the simulations. On the basis of the simulations the site of high-latitude reconnection was polarward of the Polar location when Polar encountered the reconnection layer. The plasma velocity seen by Polar is in good agreement with the simulation results

A key question regarding the interpretation of April 11, 1997, observations and the simulation results is why the flow nearly stagnates in the reconnection layer sunward of the reconnection site. Apparently, this is different from typical observations of the reconnection layer in the tail or at the dayside magnetopause. In the latter cases one observes flows in the current layer that point away from the reconnection site. Because the current layer on either side of the reconnection site must be a rotational discontinuity one can use Walen's theorem to show that these flows are indeed consistent with reconnection. This technique has been used extensively in the past to infer reconnection at the dayside magnetopause [*Paschmann et al.*, 1979; *Sonnerup et al.*, 1981; *Phan et al.*, 1996; *Scudder et al.*, 1999] where suitable observations were available.

The key difference between reconnection at the dayside magnetopause and in the tail versus high-latitude reconnection is the

presence of flow shear and pressure gradients in the latter case. On the magnetosheath side, sunward of the reconnection site, the magnetosheath flow is opposed to the outflow from the reconnection site. Apparently, the momentum flux of the magnetosheath flow and the tailward pressure gradient force roughly balance the **JxB** force in the reconnection layer that would otherwise cause sunward acceleration of the plasma emanating from the reconnection site. This picture is consistent with the simulation result that shows that the reconnection site is not stationary. Because of the flow stagnation plasma piles up sunward of the reconnection site, as plasma is both added from the magnetosheath and from the reconnection site. In reaction to this plasma pile up, the reconnection site must move tailward. As the reconnection site moves tailward, a new X line forms on the sunward side, leading to the formation of a plasmoid or flux rope, which carries away some of that stagnant plasma. This process repeats itself periodically and is reminiscent of tail reconnection where plasmoids and flux ropes also carry away plasma that has been piled up and no other way to go. Polar always remains sunward of any of the X lines and thus only observes the stagnant plasma. A full confirmation of this scenario requires observation further tailward which the Cluster II mission will hopefully provide.

We should note that this picture is rather simple and may certainly need refinement. First, the flow stagnation depends on the force balance between pressure gradients, magnetosheath momentum flux, and the reconnection **JxB** force. Thus the process strongly depends on solar wind and IMF parameters. It is conceivable that different conditions may lead to earthward flows or just decelerated tailward flows. Second, it is well known that the plasma in the vicinity of a reconnection site is far from thermodynamic equilibrium, i.e., a kinetic treatment is warranted [*Cowley*, 1982; *Smith and Lockwood*, 1996]. However, for simple pressure balance arguments as ours the MHD treatment may still suffice because most forces would not change under a kinetic treatment, except for the pressure gradient that one would need to replace by the divergence of an appropriate pressure tensor. Detailed analysis of the observed distribution functions and hybrid kinetic simulations may provide a more accurate picture.

7. Summary

We present a correlative study of the solar wind interaction with the magnetosphere using in situ observations of polar cusp and surrounding region, ground-based and low-altitude spacecraft polar cap observations, and global MHD simulations during an extended period of strongly northward IMF on April 11, 1997. Polar entered a region with dense magnetosheath-like plasma above the northern cusp. The magnetic field rotated from lobe-like field orientation to magnetosheath-like orientation upon entry. Data from multiple instruments on Polar showed that the signatures were not caused by Polar going into the magnetosheath proper. Rather, the observations can be interpreted as Polar entering into the reconnection layer and crossing the current layer thereof. The magnetosheath-like field lines encountered by Polar have just reconnected poleward of the polar cusp in the north. The reversed ionospheric convection patterns derived from the assimilative mapping of ionospheric electrodynamics (AMIE) technique show reversed convection over the polar cap due to high-latitude reconnetion throughout the whole interval. MHD simulations were performed using solar wind parameters observed by Wind, supporting the cusp reconnection interpretation. However, the observed current sheet is much thinner than predicted by the MHD simulation resulting in much faster crossings of the current sheet.

The event on April 11, 1997, presents a good example of what we can learn about processes at the magnetospheric boundary in the solar wind-magnetosphere interaction from correlative solar wind, in situ observations, ground-based and low-altitude spacecraft data, and global MHD model. As the next solar maximum is approaching, we expect the Polar spacecraft will have more chances to probe the high-latitude magnetopause boundary layer and more details of high-latitude reconnection process are expected to be revealed in future correlative studies.

Acknowledgments. We wish to thank K. Ogilvie for providing data from Wind Solar Wind Experiment, R. Lepping for data from Wind Magnetic Fields Investigation, J. Scudder for HYDRA data and W. K. Peterson for TIMAS data. G. Le and C. T. Russell were supported by the National Aeronautics and Space Administration (NASA) under research grant NAG5-7721. J. Raeder was supported by the National Science Foundation (NSF) under research grant ATM 97-13449. G. Lu was supported by NASA ISTP and SEC Guest Investigator programs. S. Petrinec was supported by NASA ISTP programs. F. Mozer was supported by NASA under research grant 19982924.

Hiroshi Matsumoto thanks T. Mukai and another referee for their assistance in evaluating this paper.

References

Berchem, J., J. Raeder, and M. Ashour-Abdalla, Magnetic flux ropes at the high-latitude magnetopause, *Geophy. Res. Lett., 22*, 1189-1192, 1995.

Burke, W. J., M. C. Kelley, R. C. Sagalyn, M. Smiddy, and S. T. Lai, Polar cap electric field structures with northward interplanetary magnetic field, *Geophys. Res. Lett., 6*, 21-24, 1979.

Cowley, S. W. H., The causes of convection in the Earth's magnetosphere: A review of developments during IMS, *Rev. Geophys., 20*, 531-565, 1982.

Dungey, J. W., Interplanetary magnetic field and auroral zones, *Phys. Rev. Lett., 6*, 47-48, 1961.

Frank, L. A., Plasmas in the Earth's polar magnetosphere, *J. Geophys. Res., 76*, 5202-5219, 1971.

Fuselier, S. A., B. J. Anderson, and T. G. Onsager, Electron and ion signatures of field line topology at the low-shear magnetopause, *J. Geophys. Res., 102*, 4847-4863, 1997.

Fuselier, S. A., K. J. Trattner, and S. M. Petrinec, Cusp observations of high- and low-latitude reconnection for northward interplanetary magnetic field, *J. Geophys. Res., 105*, 253-266, 2000.

Gosling, J. T., M. F. Thomsen, S. J. Bame, R. C. Elphic, and C. T. Russell, Observations of reconnection of interplanetary and lobe magnetic field lines at the high-latitude magnetopause, *J. Geophys. Res., 96*, 14,097-14,106, 1991.

Gosling, J. T., M. F. Thomsen, G. Le, and C. T. Russell, Observations of magnetic reconnection at the lobe magnetopause, *J. Geophys. Res., 101*, 24,765-24,773, 1996.

Harvey, P., et al., The Electric Field Instrument on the Polar satellite, *Space Sci. Rev., 71*, 583-596, 1995.

Heikkila, W. J., and J. D. Winningham, Penetration of magnetosheath plasma to low latitudes through the dayside magnetospheric cusps, *J. Geophys. Res., 76*, 883-891, 1971.

Kessel, R. L., S.-H. Chen, J. L. Green, S. F. Fung, S. A. Boardsen, L. C. Tan, T. E. Eastman, J. D. Craven and L. A. Frank, Evidence of high-latitude reconnection during northward IMF: Hawkeye observations, *Geophys. Res. Lett., 23*, 583-586, 1996.

Knipp, D. J., A. D. Richmond, B. Emery, N. U. Crooker, O. de la Beaujardiere, D. S. Evans, and H. W. Kroehl, Ionospheric convection response to changing IMF direction, *Geophys. Res. Lett., 18*, 721-724, 1991.

Le, G., C. T. Russell, and J. T. Gosling, Structure of the magnetopause for low Mach number and strongly northward interplanetary magnetic field, *J. Geophys. Res., 99*, 23,723-23,734, 1994.

Le, G., C. T. Russell, J. T. Gosling, and M. F. Thomsen, ISEE observations of low latitude boundary layer for northward interplanetary magnetic field: Implications for cusp reconnection, *J. Geophys. Res., 101*, 27,239-27,249, 1996.

Lepping, R. P., et al., The Wind magnetic field investigation, *Space Sci. Rev., 71*, 207-229, 1995.

Lu, G., et al., Interhemispheric asymmetry of the high-latitude ionospheric convection pattern, *J. Geophys. Res., 99*, 6491-6510, 1994

Maezawa, K., Magnetospheric convection induced by positive and negative z component of the interplanetary magnetic field: Quantitative analysis using polar cap magnetic records, *J. Geophys. Res., 81*, 2289-2303, 1976.

Ogilvie, K. W., et al., SWE, A comprehensive plasma instrument for the Wind spacecraft, *Space Sci. Rev., 71*, 55-77, 1995.

Paschmann, G., B. U. O. Sonnerup, I. Papamastorakis, N. Sckopke, G. Haerendel, S. J. Bame, J. R. Asbridge, J. T. Gosling, C. T. Russell, and R. C. Elphic, Plasma acceleration at the Earth's magnetopause: Evidence for reconnection, *Nature, 282*, 243-246, 1979.

Paschmann, G., B. Sonnerup, I. Papamastorakis, W. Baumjohann, N. Sckopke, and H. Luehr, The magnetopause and boundary layer for small magentic shear: Convection electric fields and reconnection, *Geophys. Res. Lett., 17*, 1829-1832, 1990.

Petrinec, S. M., and C. T. Russell, External and internal influences on the size of the dayside terrestrial magnetosphere, *Geophys. Res. Lett., 20*, 339-342, 1993.

Phan, T.-D., G. Paschmann, and B. U. O. Sonnerup, The low latitude dayside magnetopause and boundary layer for high magnetic shear, 2, Occurrence of magnetic reconnection, *J. Geophys. Res., 101*, 7817-7828, 1996.

Raeder, J., Modeling the magnetosphere for northward interplanetary magnetic field: Effects of electrical resistivity, *J. Geophys. Res., 104*, 17,357-17,367, 1999.

Raeder, J., et al., Boundary layer formation in the magnetotail: Geotail observations and comparisons with a global MHD model, *Geophys. Res. Lett., 24*, 951-954, 1997.

Raeder, J., J. Berchem, and M. Ashour-Abdalla, The Geospace Enviroment Modeling grand challenge: Results from a Global Geospace Circulation Model, *J. Geophys. Res., 103*, 14,787, 1998.

Reiff, P. H., Sunward convection in both polar caps, *J. Geophys. Res., 87*, 5976-5980, 1982.

Reiff, P. H., T. W. Hill, and J. L. Burch, Solar wind plasma injection at the dayside magnetospheric cusp, *J. Geophys. Res., 82*, 479, 1977.

Richmond, A. D., and K. Kamide, Mapping electrodynamic features of the high-latitude ionosphere from localized observations: Technique, *J. Geophys. Res., 93*, 5741-5759, 1988.

Ridley, A. J., G. Lu, C. R. Clauer, and V. O. Papitashvili, Ionospheric convection during nonsteady interplanetary magnetic field conditions, *J. Geophys. Res., 102*, 14,563-14,579, 1997.

Russell, C. T., The configuration of the magnetosphere, in *Critical Problems of Magnetospheric Physics*, edited by E. R. Dyer, pp. 1-16, Inter-Union Comm. on Sol. Terr. Phys. Secr., Nat. Acad. of Sci., Washington, D. C., 1972.

Russell, C. T., R. C. Snare, J. D. Means, D. Pierce, D. Dearborn, M. Larson, G. Barr, and G. Le, The GGS/Polar magnetic fields investigation, *Space Sci. Rev., 71*, 563-582, 1995.

Russell, C. T., J. A. Fedder, S. P. Slinker, X-W. Zhou, G. Le, J. G. Luhmann, F. R. Fenrich, M. O. Chandler, T. E. Moore, and S. A. Fuselier , Entry of the POLAR spacecraft into the polar cusp under northward IMF conditions, *Geophys. Res. Lett., 25*, 3015-3018, 1998.

Russell, C. T., G. Le, P. Chi, X-W Zhou, J.H. Shue, S. M. Petrinec, P. Song, F.R. Fenrich, and J.G. Luhmann, The extreme compression of the magnetosphere, May 4, 1998, as observed by the POLAR spacecraft, *Adv. Space Res., 25*(7/8) 1369-1375, 2000a.

Russell, C. T., G. Le, and S. M. Petrinec, Cusp observations of high- and low-latitude reconnection for northward IMF: An alternate view, *J. Geophys. Res., 105*, 5489-5495, 2000b.

Scholer, M., Asymmetric time-dependent and stationary reconnection at the dayside magnetopause, *J. Geophys. Res., 94*, 15,099-15,111, 1989.

Scudder, J., et al., HYDRA - A 3-dimensional electron and ion hot plasma instrument for the Polar spacecraft of the GGS mission, *Space Sci. Rev., 71*, 459-495, 1995.

Scudder, J. D., P. A. Puhl-Quinn, F. S. Mozer, K. W. Ogilvie, and C. T. Russell, Generalized Walen tests through Alfven waves and rotational discontinuities using electron flow velocities, *J. Geophys. Res., 104*, 19,817-19,833, 1999.

Shelley, E. G., et al., The Toroidal Imaging Mass-Angle Spectrograph (TIMAS) for the Polar mission, *Space Sci. Rev., 71*, 497-530, 1995.

Smith, M. F., and M. Lockwood, Earth's magnetospheric cusps, *Rev. Geophys., 34*, 233-260, 1996.

Song, P., and C. T. Russell, Model of the formation of the low-latitude boundary layer for strongly northward interplanetary magnetic field, *J. Geophys. Res., 97*, 1411-1420, 1992.

Song, P., C. T. Russell, R. J. Fitzenreiter, J. T. Gosling, M. F. Thomsen, D. G. Mitchell, S. A. Fuslier, G. K. Parks, R. R. Anderson, and D. Hubert, Structure and properties of the subsolar magnetopause for northward interplanetary magnetic field: Multiple-Instrument Particle Observations, *J. Geophys. Res., 98*, 11,319-11337, 1993.

Sonnerup, B. U. O., G. Paschmann, I. Papamastorakis, N. Sckopke, G. Haerendel, S. J. Bame, J. R. Asbridge, J. T. Gosling, and C. T. Russell, Evidence for magnetic field reconnection at the Earth's magnetopause, *J. Geophys. Res., 86*, 10,049-10,067, 1981.

Spreiter, J. R., A. L. Summers, and A.Y. Alksne, Hydromagnetic flow around the magnetosphere, *Planet. Space Sci., 14*, 223-253, 1966.

Tsyganenko, N. A., Effects of the solar wind conditions on the global magnetospheric configuration as deduced from data-based field models, in *Proceedings of the ICS-3 Conference on Substorms, Eur. Space Agency Spec Publ., ESA SP-389*, 181-185, 1996.

Woch, J., and R. Lundin, Magnetosheath plasma precipitation in the polar cusp and its control by the interplanetary magnetic field, *J. Geophys. Res., 97*, 1421-1430, 1992.

Zanetti, L. J., T. A. Potemra, T. Iijima, W. Baumjohann, and P. R. Bythrow, Ionospheric and Birkeland current distributions for northward interplanetary magnetic field: Inferred polar convection, *J. Geophys. Res., 89*, 7453-7458, 1984.

G. Le, Laboratory for Extraterrestrial Physics, Code 696, NASA Goddard Space Flight Center, Greenbelt, MD 20771 (Guan.Le@gsfc.nasa.gov).

G. Lu, High Altitude Observatory, National Center for Atmospheric Research, Boulder, CO 80307-3000 (ganglu@ncar.ucar.edu).

F. S. Mozer, Space Sciences Laboratory, University of California, Berkeley, CA 94720 (fmozer@apollo.ssl.berkeley.edu).

S. M. Petrinec, Lockheed Martin Advanced Technology Center, Space Physics Laboratory, Palo Alto, CA 94304-1187 (petrinec@mail.spasci.com).

J. Raeder and C. T. Russell, Institute of Geophysics and Planetary Physics, University of California, Los Angeles, CA 90095-1567 (jraeder@igpp.ucla.edu; ctrussell@igpp.ucla.edu).

(Received September 27, 1999; revised June 15, 2000;
accepted June 15, 2000.)